

# Degradation/decoloration of concentrated solutions of Orange II. Kinetics and quantum yield for sunlight induced reactions via Fenton type reagents

J. Bandara<sup>a</sup>, C. Morrison<sup>a</sup>, J. Kiwi<sup>a,\*</sup>, C. Pulgarin<sup>b</sup>, P. Peringer<sup>b</sup>

<sup>a</sup> Institute of Physical Chemistry, E.P.F.L. CH-1015, Lausanne, Switzerland

<sup>b</sup> Institute of Environmental Engineering, Bioengineering, E.P.F.L. CH-1015, Lausanne, Switzerland

Received 22 November 1995; accepted 19 February 1996

## Abstract

Light and thermal processes involving Fenton reagent are shown to be effective in the mineralization/decoloration of concentrated Orange II solutions. Light activation accelerates the observed degradation and the UV component of natural sunlight is sufficient to promote the reaction leading to the azo-dye abatement. The degradation involves dark and light steps. Kinetic information on these steps is reported. The results obtained in this study suggests that the thermodynamic potential for the redox couple in a Fenton-like reagent is not the most important factor controlling the degradation of this dye. A quantum yield of 0.10 was observed for Orange II disappearance. Decoloration of a 2.9 mM dye solution (450 mg C l<sup>-1</sup>) is achieved in less than 2 h via photo-Fenton reactions and mineralization is completed to 95% in less than 8 h. A turnover number of 4.7 was estimated for light induced processes in the model system used. Cyanuric acid added to the Fenton system suggests that besides the OH radicals, highly stable Fe-complexes in combination with H<sub>2</sub>O<sub>2</sub> are active in the abatement of this azo-dye. Near surface radical formation is shown to be important during the observed photocatalysis. No activation energy was detected during the mineralization suggesting a radical mechanism for this reaction. The quantum yields observed as a function of wavelength during Orange II disappearance corresponds in experimental error to the point-by-point addition of the absorbance of the Fe<sup>3+</sup> and H<sub>2</sub>O<sub>2</sub> solutions used in the photolysis.

**Keywords:** Orange II; Mineralization; Quantum yields; Kinetics; Action spectrum; Sunlight irradiation

## 1. Introduction

Direct photolysis has not been found to be effective in the degradation of azo-dyes [1–6]. Biological degradation is slow for many azo-dyes and in some cases, does not proceed at all [7]. In recent years there has been a growing interest to find new and better ways to clean the environment of polluting and recalcitrant materials. Azo-dyes comprise about half of all textile dyestuffs used today. About 15% is released into the environment without cleaning.

Recent studies have shown that oxidation of organic compounds by way of the Fenton reagent is useful in the degradation of this type of compound [8] and is enhanced by light irradiation. This enhancement is due to charge transfer photoredox chemistry of Fe(III) producing additional OH radicals [9]. The interest of this study is also to assess if Fenton's

chemistry is an efficient way to treat dyes compared with the more traditional methods like adsorption into activated carbon or by chemical coagulation (alumina). These last two methods are non destructive since they transfer the azo-dye (Orange II 4-(2 hydroxy-1-naphthalene) azo benzenesulfonic acid monosodium salt) from waste water to solid waste and consequently the residue needs further processing. The object of this study is fourfold: (i) to remove high concentrations of non-biodegradable Orange II found in manufacturing sites by using solar generated radiation. This approach is only now beginning to be explored for such reactions [10]; (ii) to report the effect of irradiation  $\lambda$  and light intensity on the initial rate of dye degradation; (iii) to see how the H<sub>2</sub>O<sub>2</sub> concentration affects the Fe<sup>2+</sup> generated during in the reaction and dye abatement. Concomitantly to report on Fenton reagent causing photo-oxidation of the dye or their intermediates capable of coordinating to Fe(III); and finally (iv) to elaborate some aspects of the observed mineralization related to the light activation during the reaction.

\* Corresponding address: Institute of Physical Chemistry, E.P.F.L. CH-1015, Lausanne, Switzerland.

## 2. Experimental section

### 2.1. Materials and techniques employed

Orange II Fluka, standard indicator for microscopy was used as received. Hydrogen peroxide and  $\text{FeCl}_3$  were Fluka p.a. and used without further purification.

Spectrophotometric analysis was carried out by means of a Hewlett-Packard 8452A diode array. The total organic carbon (TOC) during the reaction was monitored via a Shimadzu 500 instrument equipped with an ASI 502 automatic sample injector. High pressure liquid chromatography (HPLC) was carried out via a Varian 5500 unit. The solution gradient was regulated with a buffer consisting of ammonia acetate ( $30 \text{ mmol l}^{-1}$ ) and methanol in an inverse phase column (Phenomenex C-18). Signals for Orange II were detected at 282 nm with a retention time of 20.1 min. Detection of  $\text{CO}_2$  was performed via a Gow-Mac instrument using Ar as carrier gas and a Poropak column. The determination of nitrates, nitrites and sulfates was carried by ion liquid chromatography (ILC) via a Wescan ion analyzer. The column employed was a Hamilton anion PRPX-100 with a mobile phase 2 mM phthalic acid at pH 5. The ammonia ion was determined via a Tecator titrator forming the Cu-blue color and measuring the amount of this complex by spectrophotometric means.

### 2.2. Photoreactor, lamps and irradiation procedures

The irradiation of the solutions was carried out in Pyrex cylindrical flasks (60 ml volume) transmitting light at  $\lambda > 290 \text{ nm}$ . Two types of lamps were used: a) an Hanau Suntest solar simulator with  $90 \text{ mW cm}^{-2}$  and b) Xe-arc Osram lamps of 44 and  $135 \text{ mW cm}^{-2}$ . The radiation from these lamps was filtered through a circulating water cuvette ( $d = 6 \text{ cm}$ ) which reduced incidental warming by infrared radiation to no greater than  $\approx 2$  degrees. The radiant flux was measured with a power meter from Yellow Springs, CO, USA. Chemical actinometry was carried out by means of an Aberchrome 540 chemical actinometer in the range 310–545 nm. After photocoloration, the solution can be bleached by exposure to white light and reused. The actinometer was irradiated under conditions similar to those of the photoreaction used. This eliminated the need to make corrections for the reflectance and non-uniformity of the incident light beam. The determination of quantum yields at various wavelengths was carried out by way of a high intensity Bausch and Lomb monochromator biased at 300 nm. The incident beam on the solution had an area of  $1 \text{ cm}^2$ .

## 3. Results and discussion

### 3.1. Assessment of the photocatalytic potential of Fenton-like systems in the degradation of Orange II

Fig. 1 presents the TOC vs. reaction time for a solution of Orange II (2.9 mM) adding  $\text{H}_2\text{O}_2$  (10 mM) and  $\text{Fe}^{3+}$  (0.92

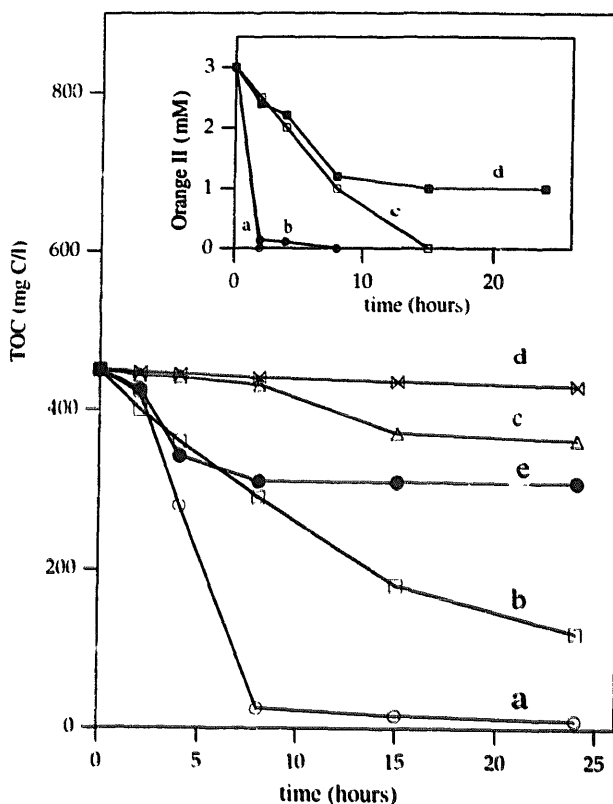


Fig. 1. TOC for a solution of Orange II (2.9 mM) adding Fenton reagent  $\text{M}^{3+}$  (0.92 mM) and  $\text{H}_2\text{O}_2$  (10 mM) as a function of time: a,  $\text{Fe}^{3+}$  (light); b,  $\text{Cu}^{2+}$  (light); c,  $\text{Cr}^{2+}$  (light); d,  $\text{Mn}^{2+}$  (light); e,  $\text{Fe}^{3+}$  (dark). The insert shows the disappearance of Orange II with: a,  $\text{Fe}^{3+}$  (light); b,  $\text{Fe}^{3+}$  (dark); c,  $\text{Cu}^{2+}$  (light); d,  $\text{Cu}^{2+}$  (dark).

mM) in dark and light induced reactions via a Suntest solar simulator. The addition of  $\text{H}_2\text{O}_2$  was carried out hourly by injecting  $40 \mu\text{l}/40 \text{ ml}$  solution. Concentrated solutions have been used in Fig. 1 since concentrations of ( $0.5 \text{ g l}^{-1}$ ) are found in the effluents of industrial sites. To find a chemical system and the most favourable conditions for the azo-dye abatement at these relatively high concentrations was the aim in Fig. 1. After a series of preliminary experiments involving optimization of the  $\text{H}_2\text{O}_2$  and metal ion, Fig. 1 shows that different transition metals render different degradation kinetics and reaction efficiencies for the reaction under study. For  $\text{Fe}^{3+}$ ,  $\text{Cr}^{2+}$ ,  $\text{Cu}^{2+}$  and  $\text{Mn}^{2+}$  ions, runs in irradiated solutions are shown in Fig. 1 as traces a, b, c, and d respectively. Trace e,  $\text{Fe}^{3+}$  reports the most interesting result since up to 95% was mineralized within 8 h and full mineralization was reached within 24 h. The insert in Fig. 1 shows the HPLC results for the  $\text{Fe}^{3+}$  and  $\text{Cu}^{2+}$  catalyzed disappearance in light and dark reactions. It is readily seen that in the  $\text{Fe}^{3+}$ -mediated reaction under light, Orange II disappearance is observed in less than 1 h. Dark runs show a  $>96\%$  decrease for the Orange II in during the first hour, the rest being completely decomposed in up to 4 h. Light processes involving  $\text{Cu}^{2+}$  show complete abatement of the azo-dye in 8 h, while in the dark, as much as 66% remains even after 24 h reaction.

The TOC decreases in Fig. 1 show the same kinetics for dark and light induced reactions for  $\text{Fe}^{3+}$ -mediated degradation during the first two hours of reaction. Furthermore, runs have been carried out allowing a 2 h dark reaction and only then irradiating the solution with the Suntest solar simulator. The observed TOC decrease was the same as if irradiation had been applied from the beginning. This shows a dark (thermal) initial step limiting the reaction kinetics. Only after this initial period would light accelerate the reaction compared to runs in the dark.

In preliminary experiments using HPLC techniques, the appearance of several aromatic compounds has been observed. The splitting of the  $-\text{N}=\text{N}-$  bond led in oxidizing media to para-sulfo phenol and 1,2 dihydroxynaphthalene and other intermediates. Only in the later stages of the photodegradation (>4 h) do aliphatic intermediates begin to appear in the HPLC spectrogram in meaningful amounts [11]. In this insert, degradation mediated by  $\text{Fe}^{3+}$  in the dark and under light (traces a, b) and by  $\text{Cu}^{2+}$  (traces c, d) are shown since they represent the fastest degradations. The last slow photodegradation step observed after 8 h (Fig. 1) shows the difficulty of converting the N-atom associated with the Orange II into oxidized nitrogen compounds (see end of text). Slow photocatalytical degradations involving C-N bonds of aliphatic compounds (formamide) have been reported recently [12]. Fig. 1 also shows in traces b, c and d that using  $\text{Cr}^{2+}$ ,  $\text{Cu}^{2+}$  and  $\text{Mn}^{2+}$  in the same concentration as  $\text{Fe}^{3+}$  ions in the Fenton system had a lesser effect on the Orange II mineralization. Therefore the potentials alone for the series  $\text{Fe}^{3+}/\text{Fe}^{2+}$  0.77 V;  $\text{Cr}^{3+}/\text{Cr}^{2+}$  -0.41 V;  $\text{Cu}^{2+}/\text{Cu}^{1+}$  0.15 V;  $\text{Mn}^{3+}/\text{Mn}^{2+}$  -1.5 V indicating that the thermodynamic factors affecting the catalysis are not the most

important factors controlling the kinetics reported in Fig. 1. Hydration energies, size of the solvation shells, electronic transfer factors and stereoisomerism play a controlling role in the observed photocatalysis. Therefore, simply on thermodynamic grounds the results observed for the photodegradation (Fig. 1) cannot be explained by the values of the potentials for the series outlined above [13].

The overall kinetics for a  $\text{Fe}^{3+}$ -mediated photodegradation as reported in Fig. 1 is not simple first order or sigmoidal. Detailed study of the intermediates [11] will allow us to establish the individual rates for the appearance and degradation of intermediates species and integrate these rates into an overall constant in this time period. A quantum yield of 0.10 (in 10%) was found for Orange II disappearance (see HPLC insert in Fig. 1). A Suntest simulator with an overall white light output of  $3.2 \times 10^{16}$  photons  $\text{s}^{-1}$  was used having an output in the range of  $280 < \lambda < 800$  nm. A turnover number of 4.7 was estimated defining this number as the mg of dye abated per hour per mg of  $\text{H}_2\text{O}_2$  under light irradiation. Fig. 1 also shows a slow final mineralization step taking place for Orange II between 8 and 24 h.

Adding a solution 10 mM of cyanuric acid allowed the elimination of this last step in the degradation as shown in Fig. 2. In effect the degradation of Orange II with  $\text{Fe}^{3+}/\text{H}_2\text{O}_2$  decreases by about 75% when isopropanol or methanol (0.3 to 1 M) were used as  $\text{OH}$  radical scavengers [1-4,16]. Cyanuric acid would then provide a degradative route besides the  $\text{OH}$  radical. This second channel would be the Fe complex in combination with  $\text{H}_2\text{O}_2$  acting within the same mechanistic framework as the Fenton reagent (see Fig. 1 and Fig. 2). The Orange II-Fe cyanuric system could be recycled after 8 h adding new Orange II each time. Fe(III) would be preferred as a chelating agent in basic media, but this is not possible due to the iron precipitation at high pH values.

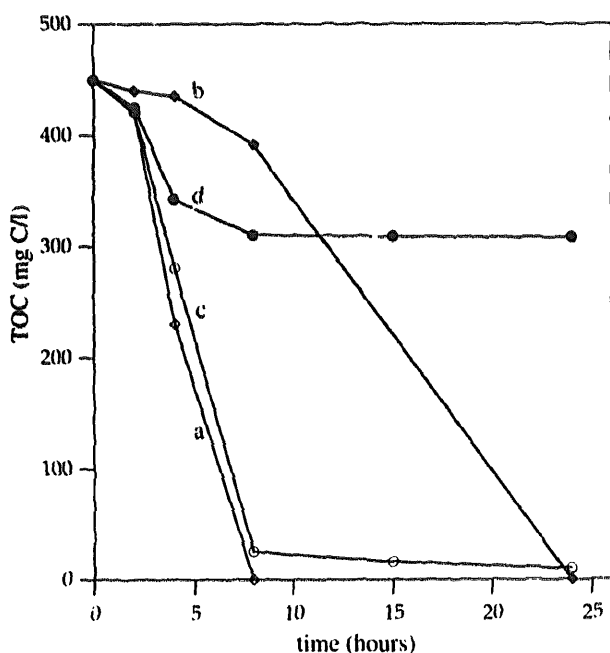
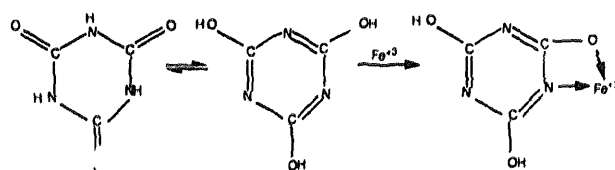


Fig. 2. TOC decrease vs. time for a solution with the same make up as in Fig. 1 with: a,  $\text{Fe}^{3+}$  cyanuric acid (10 mM) (light); b, as a but dark; c, as a but no cyanuric acid (light); d, as c but dark.



Highly stable Fe(III) complexes have been reported for a variety of aromatic compounds [18]. Conventional knowledge in the field suggests [1-6] that  $\text{OH}$  Fenton generated radicals may be the dominant reactant in (Eqs. 1-5, see below). Nevertheless the present results show that Fe(III) complexes in combination with  $\text{H}_2\text{O}_2$  (nucleophilic type addition) are additional Fenton-like reagents capable of reacting efficiently with organic substrates [18,19].

In separate experiments it was observed that the Fenton reagent does not degrade the cyanuric acid.  $\text{TiO}_2$  based systems have been reported to be unable to degrade cyanuric acid under light [17].

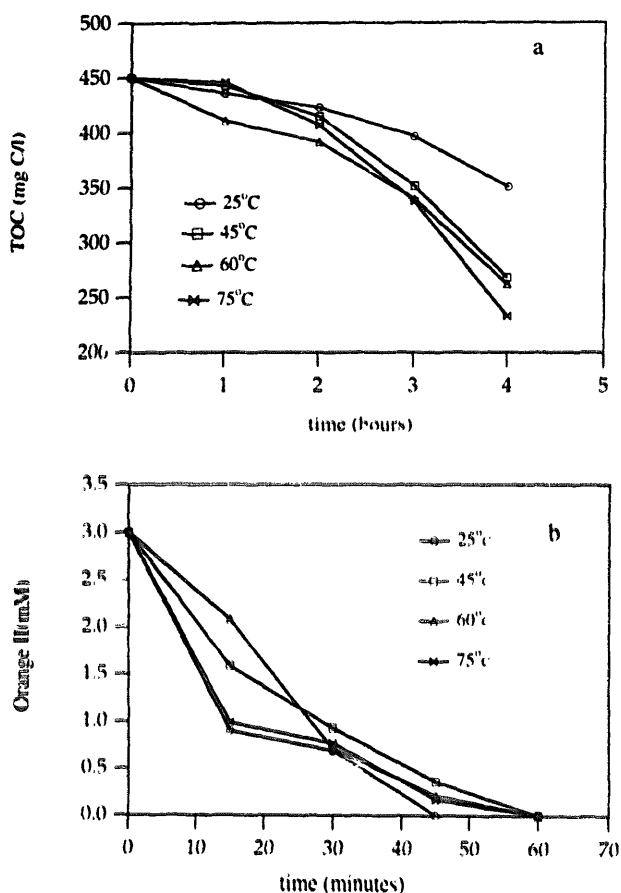


Fig. 3. (a) TOC decrease vs. time for a solution with the same make up as in Fig. 1 as a function of temperature. Light source Suntest simulator (90 mW cm<sup>-2</sup>); (b) Orange II disappearance vs. time as a function of temperature (Suntest).

### 3.2. Nature of the near-surface radical reactions active in the degradation

The overall radical mechanism postulated by Eqs. (1)–(3) (see below) could be substantiated by experimental observations in Fig. 3a. Radical reactions in the relatively narrow temperature range presented do not need any activation energy. A raise in temperature therefore should not influence the observed kinetics as is confirmed in Fig. 3a. The disappearance of Orange II is seen also to be temperature independent as shown in Fig. 3b.

The TOC decrease was measured in Fig. 4 for a solution containing Orange II (2.9 mM), Fe<sup>3+</sup> (0.92 mM) and H<sub>2</sub>O<sub>2</sub> (10 mM) at pH 3 under experimental conditions during the irradiation. The solutions were irradiated in Pyrex flasks by means of Suntest simulator (90 mW cm<sup>-2</sup>) and the degradation results for a surface-to-volume ratio (*s/v*) of 5.90 (10 ml) solution in a 60 ml flask compared with the results obtained for irradiations using 20 ml (*s/v*) 2.06 and 40 ml (*s/v*) 1.34 in the same reaction vessel. The results are plotted in Fig. 4. A more favorable photochemical reaction is observed when less volume was used in the cylindrical reac-

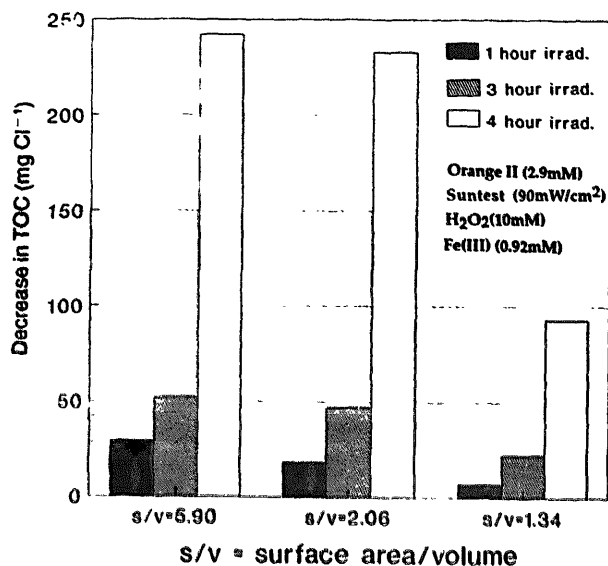
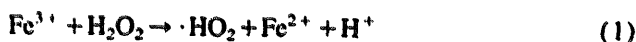


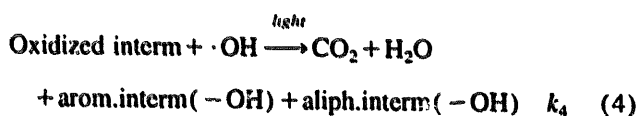
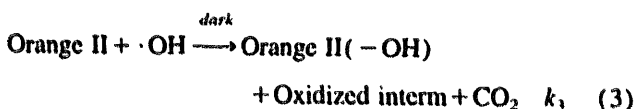
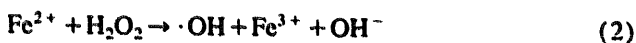
Fig. 4. Influence of the surface-to-volume ratio on the TOC decrease with time. Cylindrical flask used during irradiations.

tor. Therefore, near surface radicals are shown to play an important role in the observed degradation.

That three distinct kinetic steps are taking place during degradation can readily be seen by inspection of Fig. 1. This observation and the material presented in Figs. 1–4 allows us to suggest an overall reaction mechanism along the conventional framework of Fenton reactions



with Fe<sup>2+</sup> ion-producing  $\cdot\text{OH}$  radicals



The rate constant *k* in steps 3, 4 and 5.

$$\text{rate} = -d\text{TOC}/dt = k(\text{mg Cl h}^{-1}) \quad (6)$$

The three distinct steps in Fig. 1 show:  $k_4 > 5 k_3$  and  $k_4 > 140 k_5$ . Orange II disappearance by HPLC is much faster than the observed mineralization leading to aromatic and aliphatic intermediates. The reaction rate (see insert) can be written:

$$\text{rate} = dC_{\text{Orange II}}/dt = kC_{\text{Orange II}} \quad (7)$$

and the degradation features for concentrated solutions of Orange II up to saturation will be shown later in the text (Fig. 4). The effect of light irradiation on the degradation rate (Fig. 1) is in part due to the known photoreduction of Fe<sup>3+</sup> to Fe<sup>2+</sup> continuously producing new  $\cdot\text{OH}$  radicals from

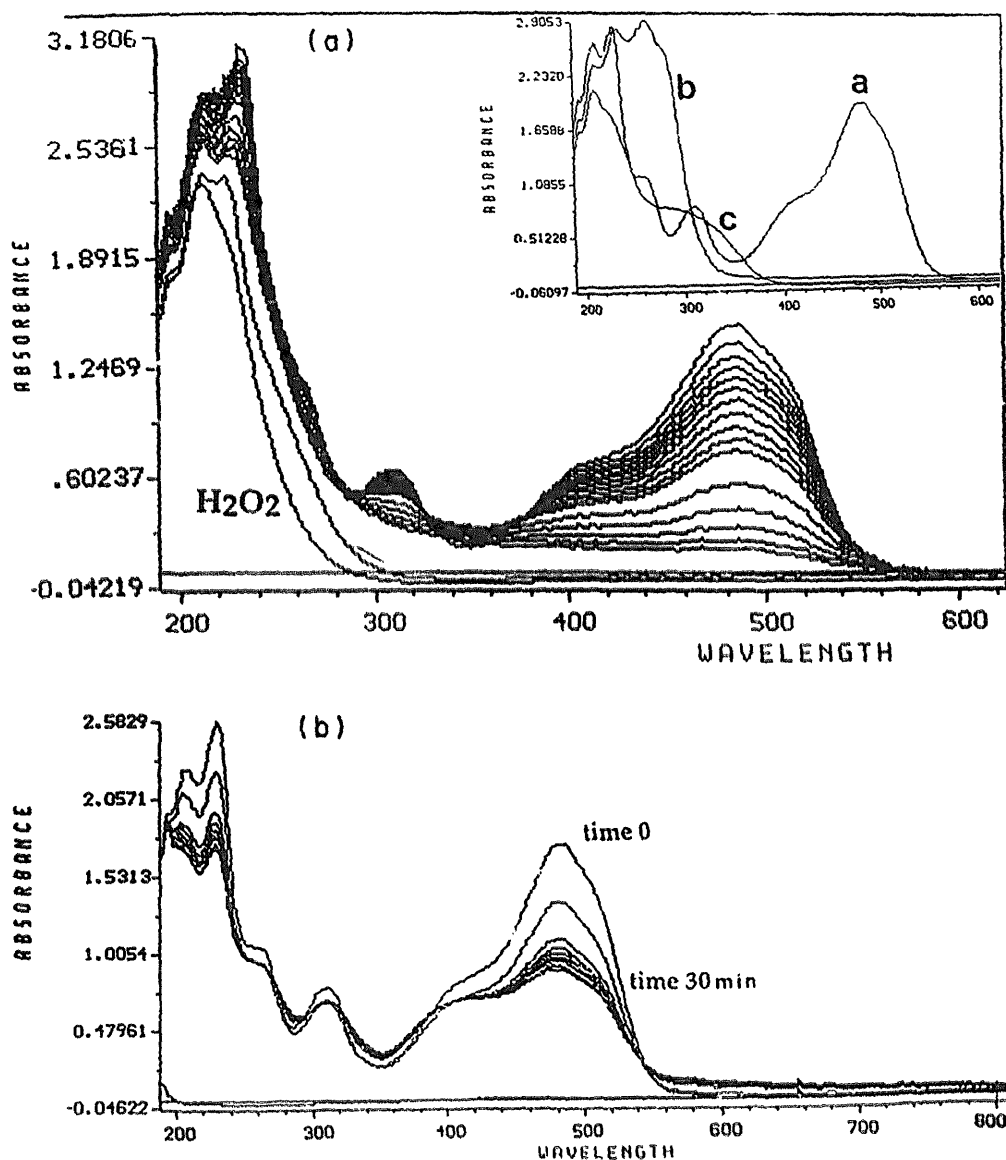


Fig. 5. (a) Spectral observations for the solution used in Fig. 1 before and after 1 h. Photolysis was carried out with a Suntest (90 mW  $\text{cm}^{-2}$ ). Traces were taken at 10 min intervals. The insert shows the spectra of a, Orange II (2.9 mM); b, Pyrex flask used; and c,  $\text{Fe}^{3+}$  (0.92 mM). (b) Spectral observations in the time interval marked for the solution used in (a) but in the absence of  $\text{H}_2\text{O}_2$ .

$\text{H}_2\text{O}_2$  [14,15]. In the dark the results show the reaction being retarded after the initial conversion of  $\text{Fe}^{3+}$  to  $\text{Fe}^{2+}$ .

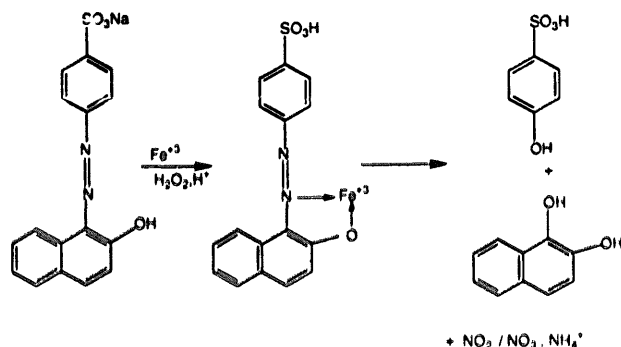
### 3.3. Photoinduced decoloration of concentrated Orange II solutions via Fenton reagent

Fig. 5a shows the decoloration/degradation of a solution Orange II (2.9 mM) when  $\text{Fe}^{3+}$  (0.9 mM) and  $\text{H}_2\text{O}_2$  (10 mM) were added and the solution irradiated with the solar simulator. It is readily seen that decoloration takes place within 1 h. The spectral observations reported in Fig. 5a were made at 4 min intervals. During photolysis a cutoff filter was used in Fig. 5a (pyrex cell  $\lambda > 295 \text{ nm}$ ) to ensure that the OH radicals originating directly from the  $\text{H}_2\text{O}_2$  hydrolysis

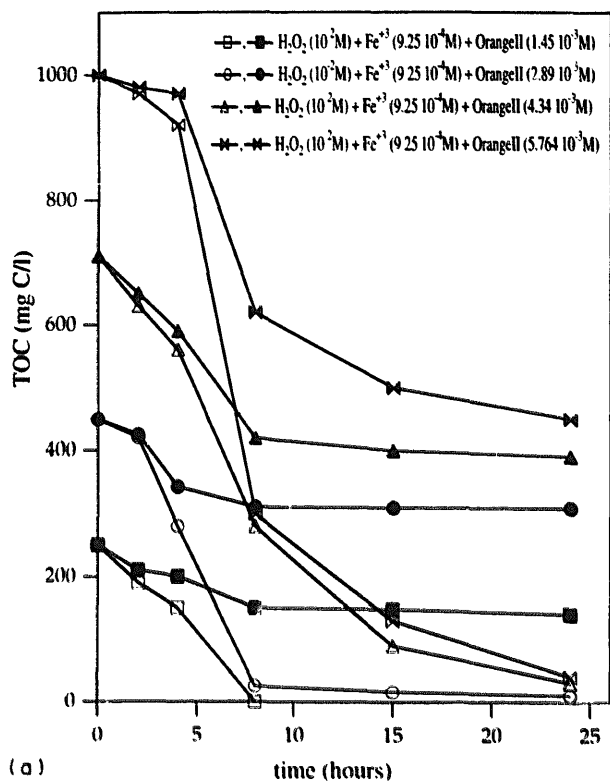
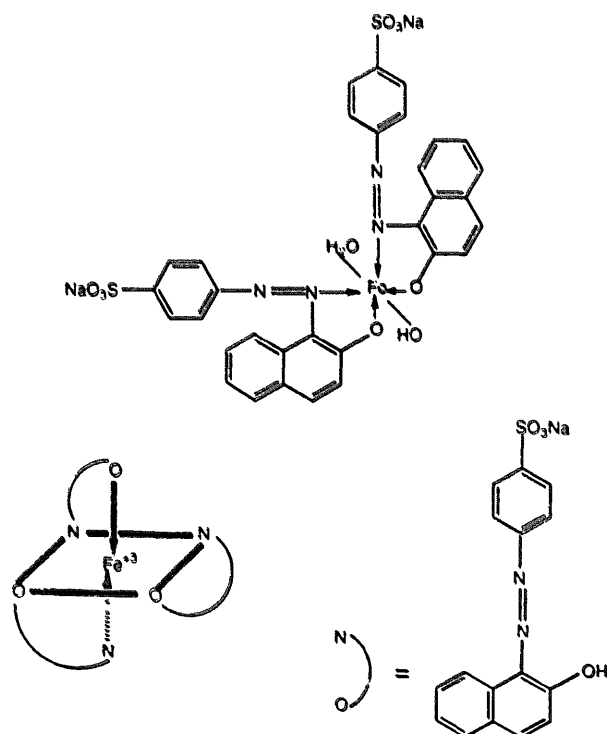
are not the source of the radicals in Eqs. (1)–(3) but Fenton related reagents and/or complexes in combination with  $\text{H}_2\text{O}_2$  are responsible for the observed decoloration. Photolysis of the azo-dye adding only  $\text{H}_2\text{O}_2$  did not induce degradation ( $\lambda > 305 \text{ nm}$ ) confirming the stability of this commercial textile dye towards strong oxidants in the visible region.

The insert in Fig. 5a presents, in trace a, the spectra of a solution of Orange II (2.9 mM). Traces b and c present the spectra observed of the Pyrex reaction vessel and  $\text{FeCl}_3$  (0.9 mM) used. Fig. 5b presents in the absence of  $\text{H}_2\text{O}_2$  the photolysis at pH 3 in air for the solution used in Fig. 5a. The experimental results show that the initial  $\text{Fe}^{3+}$  has been used up after 30 min. Therefore, light has no promoting effect on the decoloration when  $\text{Fe}^{3+}$  has been exhausted.

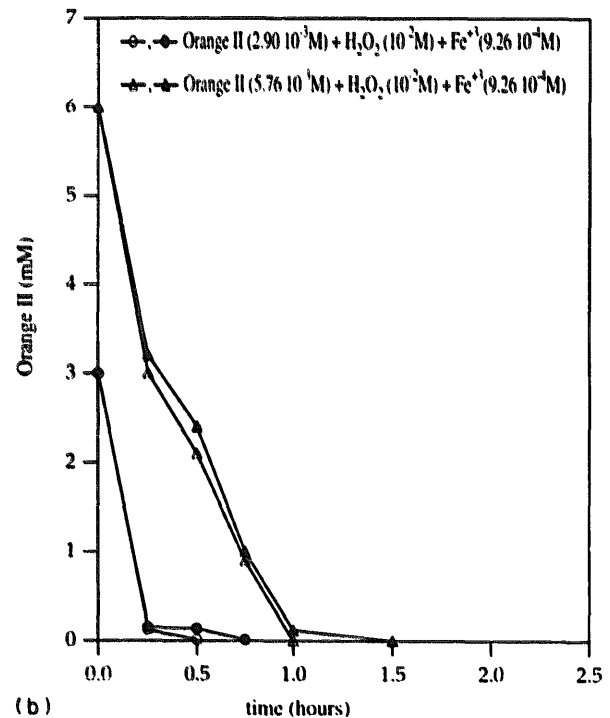
The complexation of Orange II with  $\text{Fe}^{3+}$  and the subsequent cleavage of the azo-dye linkage during the photolysis in the presence of  $\text{H}_2\text{O}_2$  with the formation of para-sulpho-phenol and 1,2 dihydroxy-naphthalene has been obtained as a preliminary result during the identification of intermediates [11].



This is consistent with the observations reported in Fig. 5 since the azo-linkages absorb light of wavelength  $> 300$  nm. The reported decrease in the dye absorbance above this wavelength reflect the azo-linkage destruction during photolysis. Later in the text the formation of oxidated nitrogen species is reported. A molar ratio of 1:1 between the azo dye and  $\text{Fe}^{3+}$  did not show any Orange II spectrum in solution, indicating full complexation of the Fe ion by the dye. Two Orange II molecules could also complex one  $\text{Fe}^{3+}$  in solution when the azo-dye was reacted with  $\text{Fe}^{3+}$  in a ratio 2:1. The possible configuration is shown below. A 3:1 Orange II:Fe complex is also seen to be partially formed by spectral observations and is schematically shown next. Our results correspond to a mixture to of the three possible complexes:



(a)



(b)

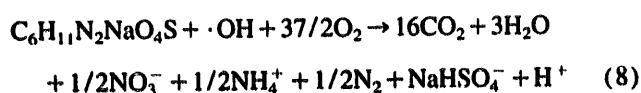
Fig. 6. (a) TOC vs. time for diverse concentrations of Orange II as marked. Open symbols, reactions under light; filled symbols, dark reactions. (b) Orange II disappearance as a function of dye concentration for the middle and highest azo-dye concentration used in Fig. 6(a). Open symbols refer to light runs and filled symbols refer to dark runs.

Fig. 6(a) shows the TOC decrease as a function of time for diverse concentrations of Orange II in light or dark. The concentrations used in traces a, b, c and d were 1.45 mM, 2.9

mM, 4.35 mM, and 5.8 mM respectively. It is readily seen in this figure that up to high dye concentrations, the classical Fenton system under light is capable of mineralizing the azo-dye. The degradation processes for the four concentrations reported in this figure under light reveal three distinct stages (see Fig. 1). The times of photomineralization are seen to increase as the solutions become more concentrated. In the dark the Orange II is seen to mineralize at the beginning rendering only a modest TOC decrease within 24 h. Fig. 6(b) shows that Orange II (HPLC) disappears within 1 h under experimental conditions for concentrations of up to  $5.75 \times 10^{-3}$  M. Since this study concerns itself with the abatement of concentrated Orange II in industrial site effluents the details of this last experiment although predictable are worth reporting.

### 3.4. Nature of the products observed during the light-induced reaction

Fig. 7(a) presents the evolution of the nitrogen and sulfo-containing products of a solution (as used in Fig. 1) during Suntest irradiation. It is readily seen in Fig. 7(a) that the decomposition of intermediate nitrite leads partly to nitrate and ammonia. When the  $-N=N-$  bond is cleaved,  $N_2$  evolution has been observed [20] in the hydrolysis of related azo-dyes [11]. This gas may account for the missing nitrogen in the mass balance for the products reported in Fig. 7(a). Besides sulfate two adjacent peaks (that may account for the rest of the sulfate) were observed in the spectrogram but could not be determined quantitatively by our ion liquid chromatograph. These results allow to write the overall stoichiometry for the mineralization of Orange II via Fenton reactions



The mechanism of formation of ammonia is known from reactions of  $H^+$  with  $NO_2^-/NO_3^-$  in acid media [4-6]. Nitrites are not cited in Eq. (8) since they are intermediate species (Fig. 7(a)) leading to ammonia, nitrates and possibly  $N_2$ .

Fig. 7(b) presents the light-induced  $CO_2$  evolution for a solution like the one used in Fig. 1 confirming the mineralization already reported by TOC measurements. In effect 95% of the stoichiometric amount of carbon was mineralized in about 8 h. The decrease in the reported amount of  $CO_2$  in Fig. 7(b) stems from the lack of meaningful pressure in the reaction vessel after this time. The insert in Fig. 7(b) reports on the  $CO_2$  evolution as a function of wavelength used. A monochromator with 5 nm slit was used for 4 h to determine each of the experimental points reported in the insert. The gas evolved was measured as in Fig. 7(a) in the upper cavity of the 60 ml cylindrical vessel containing 50 ml solution (gas phase 10 ml). It is readily seen that the shape obtained for the action spectrum for  $CO_2$  evolution strongly resembles the

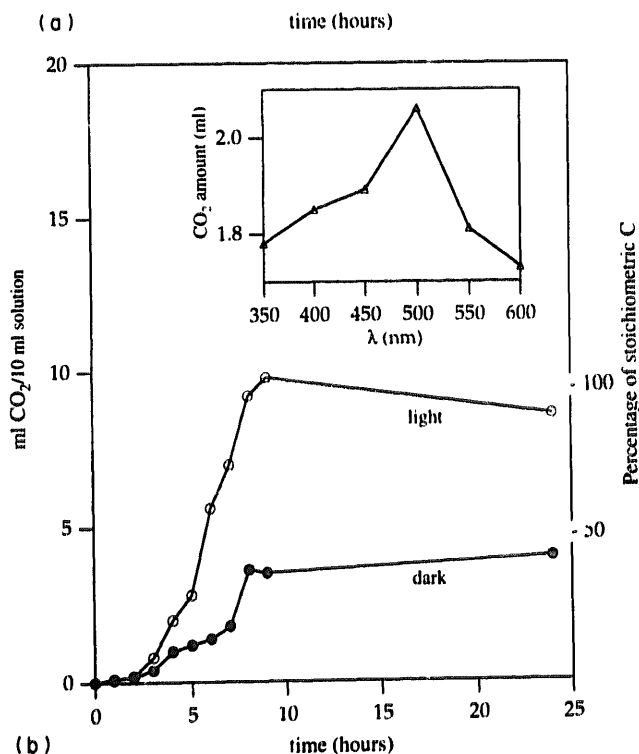
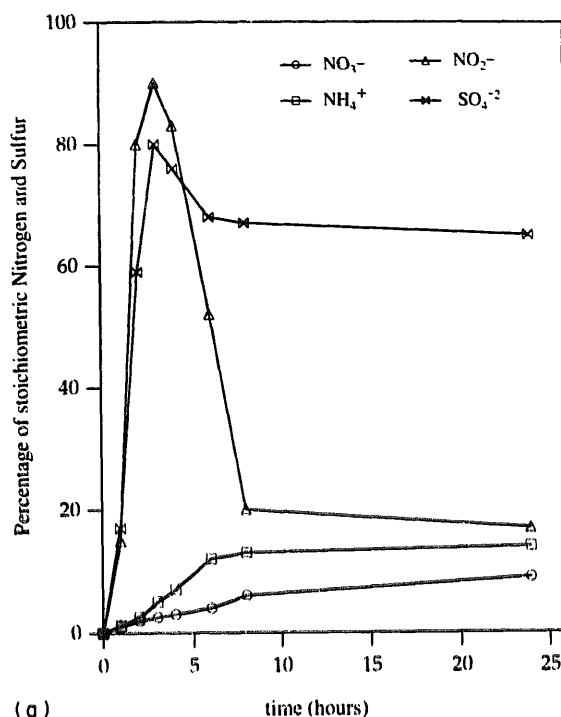


Fig. 7. (a) Nitrogen and sulfo-containing reaction products observed for runs under light when the Fenton reagent is used in Orange II degradation for the solution reported in Fig. 1. (b)  $CO_2$  evolution as a function of time for the solution used in Fig. 7(a). The evolution of this product as a function of wavelength is shown in the insert.

shape of Orange II as seen in Fig. 5(a). This experimental observation is important since the initial rates for  $CO_2$  evolution are quite different to the values reported (below in the text) for Orange II disappearance as a function of the wavelength used.

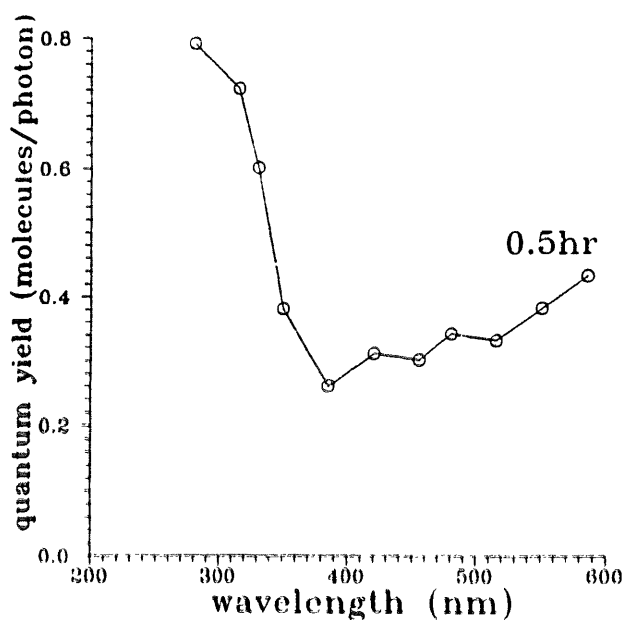


Fig. 8. Initial quantum yields for Orange II disappearance (observed by HPLC) as a function of wavelength for the same solution used in Fig. 7. The solution was Orange II (2.9 mM),  $\text{Fe}^{3+}$  (0.92 mM) and  $\text{H}_2\text{O}_2$  (10 mM). For other details see text.

### 3.5. Quantum yield of disappearance of Orange II as a function of $\lambda$

The quantum yields for Orange II disappearance as a function of  $\lambda$  are reported in Fig. 8. This dependence was studied in order to obtain information about the chromophore(s) and intermediate states involved in the homogeneous photoredox process. Monochromatic light from a Xe lamp was used between 300 and 600 nm during 0.5 and 1 h. The values were obtained by dividing the number of Orange II molecules abated (determined by HPLC) by the number of photons  $\text{cm}^{-2} \text{s}^{-1}$  used at each of the wavelengths used in Fig. 8. The actinometry used is described in Section 2. More energetic photons ( $\lambda < 380 \text{ nm}$ ) are seen to be more effective at short irradiation times during dye decomposition. The  $\text{FeOH}^{2+}$  complex has a maximum at 295 nm and the steep rise in these wavelength region for the quantum yields observed in Fig. 8 may be due to reaction (9)



The quantum yield of reaction (9) has been reported to be 0.14 at 313 nm and 0.017 at 360 nm in line with the trends shown in Fig. 8 [21]. Dissolved Fe(III) complexes photolyze with meaningful quantum yields up to 500 nm accounting for the rise of the spectrum towards longer  $\lambda$  [3]. At 1 h irradiation the appearance of intermediates (see Figs. 1-4) and product decomposition render a completely different action spectrum. More interesting is the possibility shown in Fig. 9(c) that the observed quantum yield as a function of  $\lambda$  stems from the point-by-point addition of the spectra reported in Fig. 9(a) and (b) for  $\text{H}_2\text{O}_2$  and  $\text{FeCl}_3$ . These two spectra add up to the spectrum reported for the quantum yield in

Fig. 9(c). The origin of the shape reported for the quantum yield of Orange II disappearance could therefore be explained as a function of the spectral absorption of the two solutions used in the photolysis. More interesting is to report on some preliminary work on the nature of the intermediate absorbing light after 0.5 h. Orange II,  $\text{Fe}^{3+}$  and  $\text{H}_2\text{O}_2$  were mixed as in Fig. 8 and by stop flow and spectrophotometric techniques the rise in the signals and subsequent decay were followed for 30 minutes. The rise time in the dark for the intermediate was observed to be faster and more marked than in light experiments. Under light we carried out experiments under full output of a sunlight simulator and with a filter at  $\lambda = 400 \text{ nm}$ . The intermediate species under full light output was seen

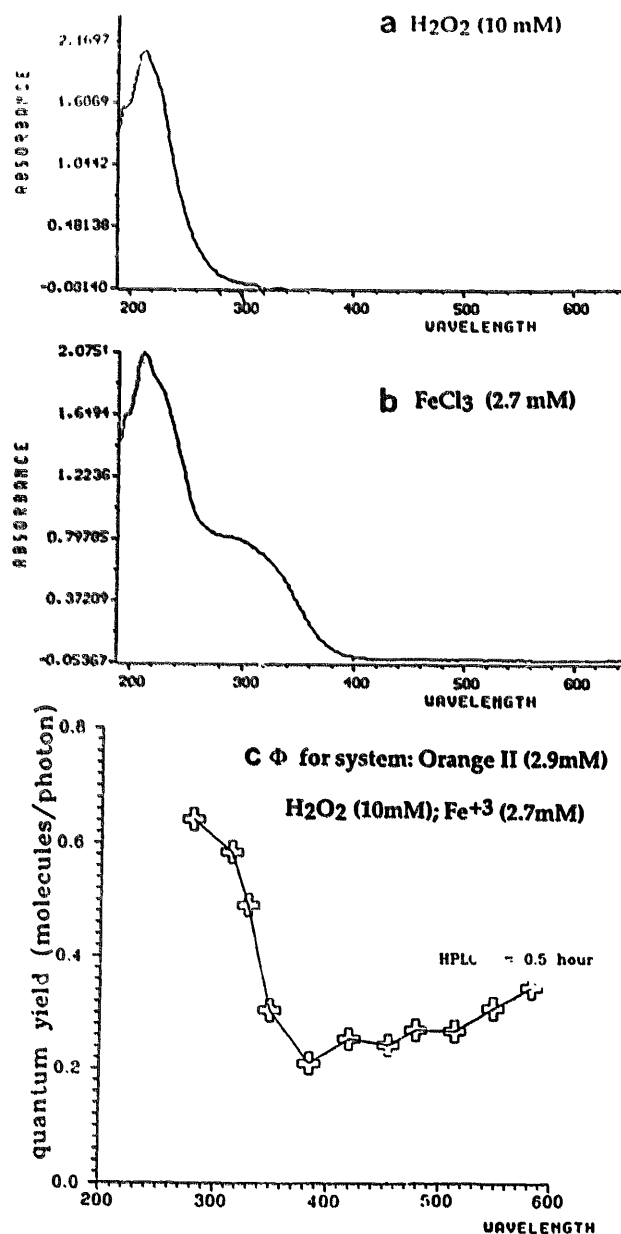


Fig. 9. Spectral observations for a,  $\text{H}_2\text{O}_2$ ; b,  $\text{FeCl}_3$ ; and c, the quantum yields as reported in Fig. 8 but indicating by the crosses the range found for the point-by-point addition of spectra a and b.

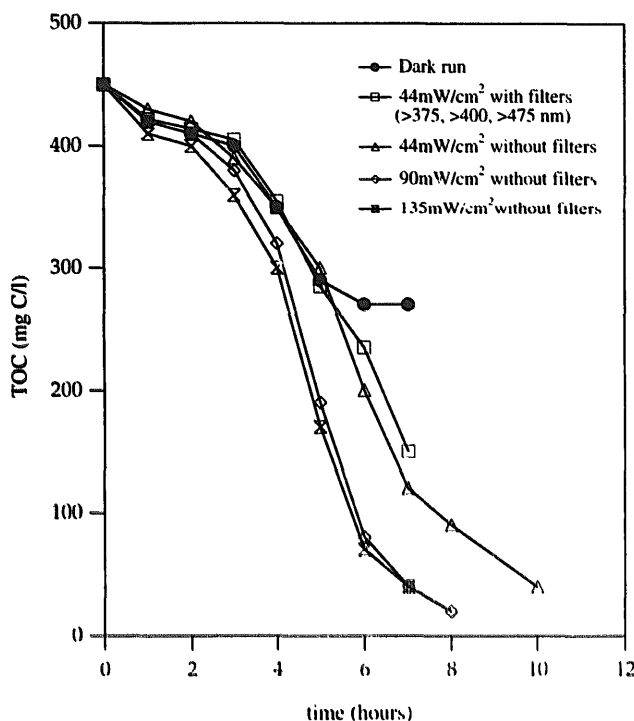


Fig. 10. TOC decrease as a function of time for solutions as used in Fig. 9 where the wavelength regions of irradiation and light intensities have been varied. For other details see text.

to rise more slowly and attain a lower total OD in time ( $\sim 50$  s) than the intermediate complex observed with the ternary system with the filter at  $\lambda = 400$  nm. Therefore a complex seems to be responsible for the observed degradation of the azo-dye that depends on two factors: a) application of light, or not, to the system; and b) the  $\lambda$  of the applied light.

### 3.6. Effect of the irradiation wavelength and light intensity on the photodegradation. Sunlight photoassisted mineralization

Fig. 10 shows the degradation in the dark and under light of a solution with the same make up as the one used in Fig. 1. The upper trace shows the dark reaction up to 6 h showing only a modest degradation. If photodegradation is carried out with a Xe lamp ( $44 \text{ mW cm}^{-2}$ ) using filters that cut the light below 345, 400 and 475 nm no difference is seen in the TOC decrease suggesting that in a narrow range of light intensities the degradation takes place via a combination of light and dark steps. One would expect the quantum yields for reaction (9) to be constant in this  $\lambda$  range as well as the direct photo-oxidation to Fe(III) reported earlier [22] and shown below by Eq. (10):



The results in Fig. 10 suggest that under experimental conditions the intermediates accelerating the degradation are produced in the dark. However, when the full light of a Xe lamp ( $44 \text{ mW cm}^{-2}$ ) and Xe lights with higher intensities were

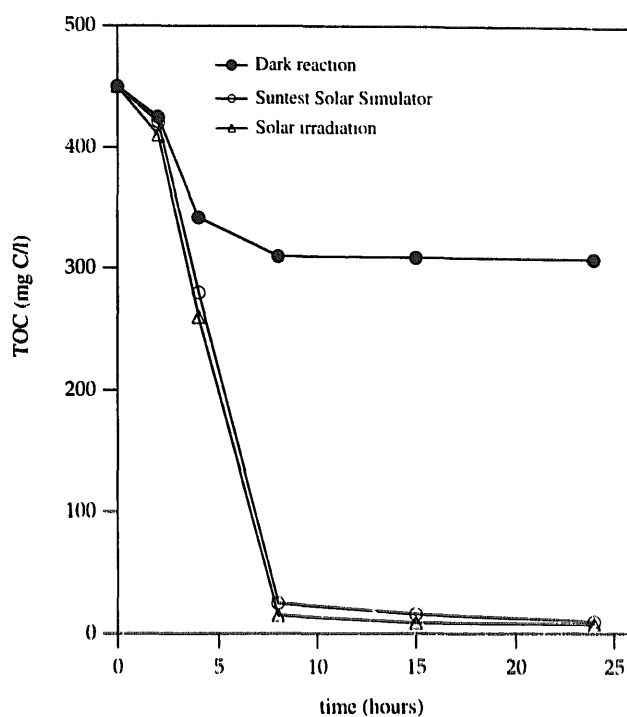


Fig. 11. TOC decrease for the solution of Orange II used in Fig. 10 when irradiated by the solar simulator ( $90 \text{ mW cm}^{-2}$ ) and by natural sunlight ( $80 \text{ mW cm}^{-2}$ ).

used ( $90 \text{ mW cm}^{-2}$  and  $135 \text{ mW cm}^{-2}$ ) they allow for a faster TOC decrease but not linearly related to the applied light intensity used.

Finally, Fig. 11 shows the sunlight-induced efficient mineralization via natural radiation on a clear day in Lausanne ( $80 \text{ mW cm}^{-2}$ ). The solution used contains Orange II ( $2.9 \text{ mM}$ ),  $\text{Fe}^{3+}$  ( $0.92 \text{ mM}$ ) and  $\text{H}_2\text{O}_2$  ( $10 \text{ mM}$  injected every hour into the reaction flask) at pH 2 in air irradiated via a Suntest solar simulator ( $90 \text{ mW cm}^{-2}$ ). The TOC decrease under light was seen to be almost the same in both cases and a lesser TOC decrease is seen to take place in the dark. Total decoloration of the azo-dye (as measured by the peak decrease at  $484 \text{ nm}$ ) was achieved in 110 minutes under sunlight irradiation at the concentrations of azo-dye ( $2.9 \text{ mM}$ ) reported in Fig. 11. Solar energy utilization when cleaning dye contaminated rivers and lakes may have therefore more than academic interest.

## 4. Conclusions

The photo-oxidation of Orange II via Fenton reagent has been reported in detail. Complete mineralization is attained with the formation of  $\text{CO}_2$ , water, nitrates, ammonia and sulfate. The initial rates of degradation and decoloration have been determined for Orange II in the presence of Fenton reagent applying simulated and natural sunlight. In less than 1 h Orange II was transformed completely into reaction intermediates. The quantum yield for this later reaction as well as for  $\text{CO}_2$  evolution is reported as a function of  $\lambda$ . Cyanuric

acid is seen to improve the dye mineralization possibly owing to an Fe cyanuric–H<sub>2</sub>O<sub>2</sub> complex which is not degraded by the Fenton reagent. Another beneficial aspect is the fact that this species absorbs light at wavelengths up to 600 nm. From the material presented in this study the Fe<sup>3+</sup>/H<sub>2</sub>O<sub>2</sub>/hν system seems to be catalytic instead of stoichiometric in iron. Further development and optimization of solar processes based on this study could be of interest for large scale environmental cleaning operations.

### Acknowledgements

This work was financially supported through grant No. EV5V-CT93-0249 from the Commission of the European Communities (OFES Contract No. 95 00 31, Bern) and through INTAS cooperation project Brussels No. 094-642.

### References

- [1] M. Hoffmann, S. Martin, W. Choi and D. Bahnemann, *Chem. Revs.*, **95** (1995) 69 (and references cited therein).
- [2] O. Legrini, E. Oliveiros and M. Braun, *Chem. Revs.*, **93** (1993) 67 (and references cited therein).
- [3] G. Helz, R. Zepp and D. Crosby (eds.), *Aquatic and Surface Chemistry*, Lewis, Boca Raton, FL, 1994 (and references cited therein).
- [4] P. Pitter and J. Chudoba, *Biodegradability of Organic Substances in the Aquatic Environment*, CRC Press, Boca Raton, FL, 1990 (and references cited therein).
- [5] J. Kiwi, C. Pulgarin, P. Peringer, M. Gratzel, *New J. Chem.*, **17** (1993) 487 (and references cited therein).
- [6] J. Kiwi, C. Pulgarin, P. Peringer, *Appl. Catal. B.*, **3** (1994) 335 (and references cited therein).
- [7] Ph. Howard, *Handbook of Environmental Degradation Rates*, Lewis, Washington DC, 1989.
- [8] E. Lipczynska-Kochany, *Environ. Tech. Lett.*, **12** (1991) 87.
- [9] Y. Sun and J. Pignatello, *Environ. Sci. Technol.*, **27** (1993) 304.
- [10] J. Bolton, *Solar Eng. Mater. Solar Cells*, **38** (1995) 543.
- [11] F. Herrera, C. Pulgarin, P. Peringer, J. Kiwi, unpublished results.
- [12] C. Maillard, Ch. Guillard, P. Pichat and M.A. Fox, *New J. Chem.*, **16** (1992) 821.
- [13] K. Rajeshwar, J. Ibanez, G. Swain, *J. Appl. Electrochem.*, **14** (1994) 1077.
- [14] G. Ruppert, R. Bauer and G. Heisler, *J. Photochem. Photobiol. A: Chem.*, **73** (1993) 75.
- [15] M. Halmann, *J. Photochem. Photobiol. A: Chem.*, **66** (1992) 215.
- [16] C. Kormann, D. Bahnemann and M. Hoffmann, *Environ. Sci. Technol.*, **22** (1988) 979.
- [17] E. Pelizzetti, V. Maurino, C. Minero, V. Carlin, E. Promauero, E. Zerbitani and M. Tosato, *Environ. Sci. Technol.*, **24**, (1990) 1559.
- [18] C. Sheu, A. Sobkowiak, L. Zhang, N. Ozbalik, D. Barton and D. Sawyer, *J. Am. Chem. Soc.*, **1** (1989) 8030.
- [19] D. Sawyer, Ch. Kang, A. Llobet and Ch. Redman, *J. Am. Chem. Soc.*, **115** (1993) 5817.
- [20] H. Zollinger in *Color Chemistry — Syntheses, Properties and Applications of Organic Dyes and Pigments*, VCH, New York, NY, 1987.
- [21] B. Faust and C. Hoigné, *J. Atmos. Environ.*, **24A** (1990) 79.
- [22] P. Braterman, A. Cairns-Smith and M. Craw, *J. Chem. Soc. Dalton Trans.*, (1984) 1441.